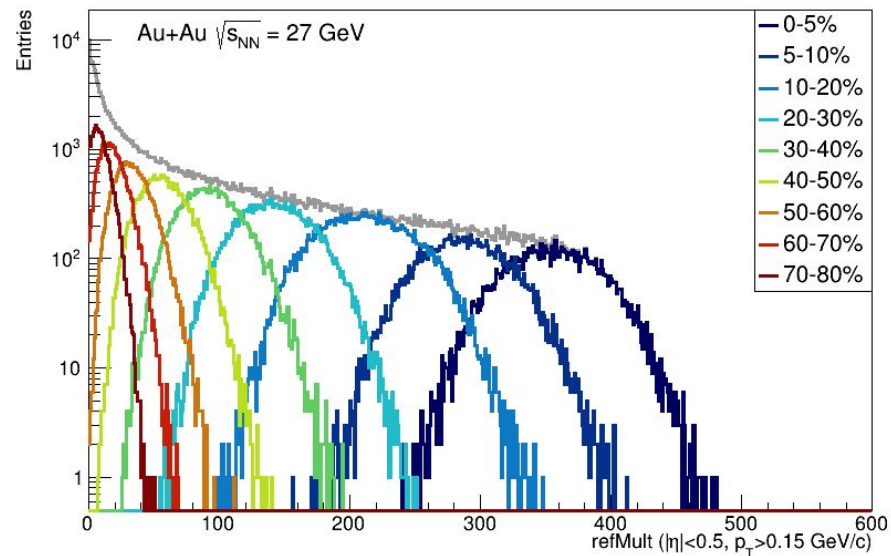
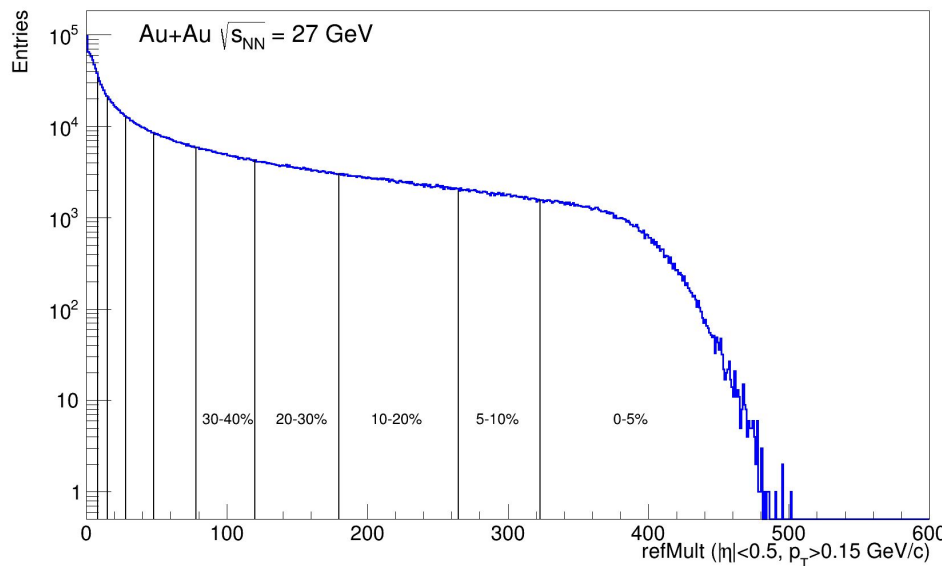


$\pi/K/p$  spectra, Au+Au,  $\sqrt{s_{NN}} = 27$  GeV

UrQMD

### Cuts for centrality calculation:

- $\pi^\pm, K^\pm, p$  (p-bar)
- $p_T > 0.15$  GeV/c
- $|\eta| < 0.5$



Au+Au, 27 GeV			
Centrality, %	Multiplicity	Percent in this bin	Cumulative percent
0-5	$322 \leq \text{mult} < 502$	0.0500505	0.0500505
5-10	$264 \leq \text{mult} < 322$	0.0495357	0.0995862
10-20	$179 \leq \text{mult} < 264$	0.100235	0.199822
20-30	$119 \leq \text{mult} < 179$	0.100627	0.300448
30-40	$77 \leq \text{mult} < 119$	0.0987935	0.399242
40-50	$47 \leq \text{mult} < 77$	0.100271	0.499513
50-60	$27 \leq \text{mult} < 47$	0.0990788	0.598592
60-70	$14 \leq \text{mult} < 27$	0.103341	0.701933
70-80	$7 \leq \text{mult} < 14$	0.0972113	0.799144

Statistics:  $\sim 2\text{M}$

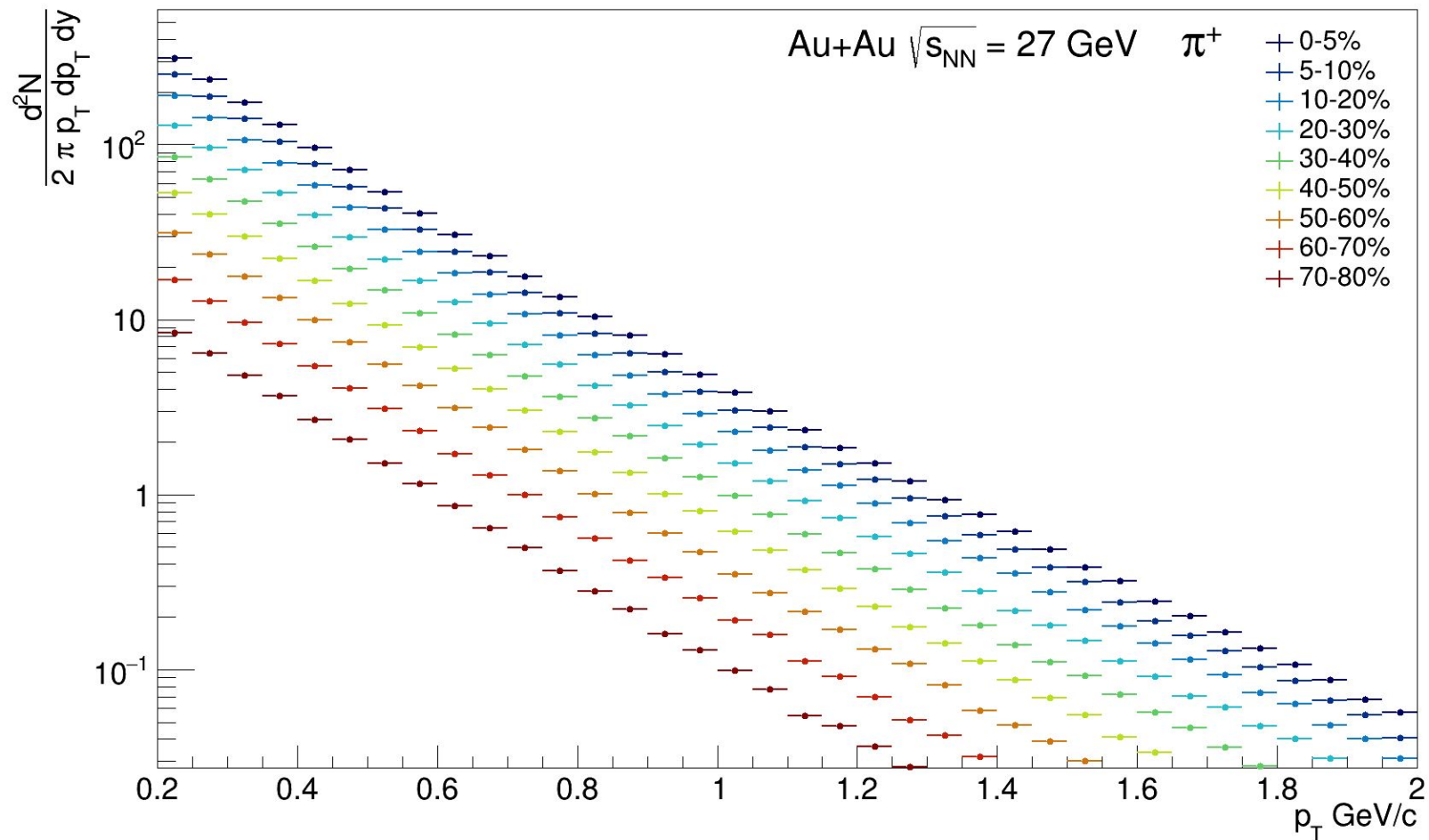
Track cuts:

- PDG ( $\pi^\pm = \pm 211$ ,  $K^\pm = \pm 321$ ,  $p$  ( $p\text{-bar}$ ) =  $\pm 2212$ )
- $|y| < 0.1$ ,
- $|\eta| < 0.5$
- $p_T > 0.2 \text{ GeV}/c$

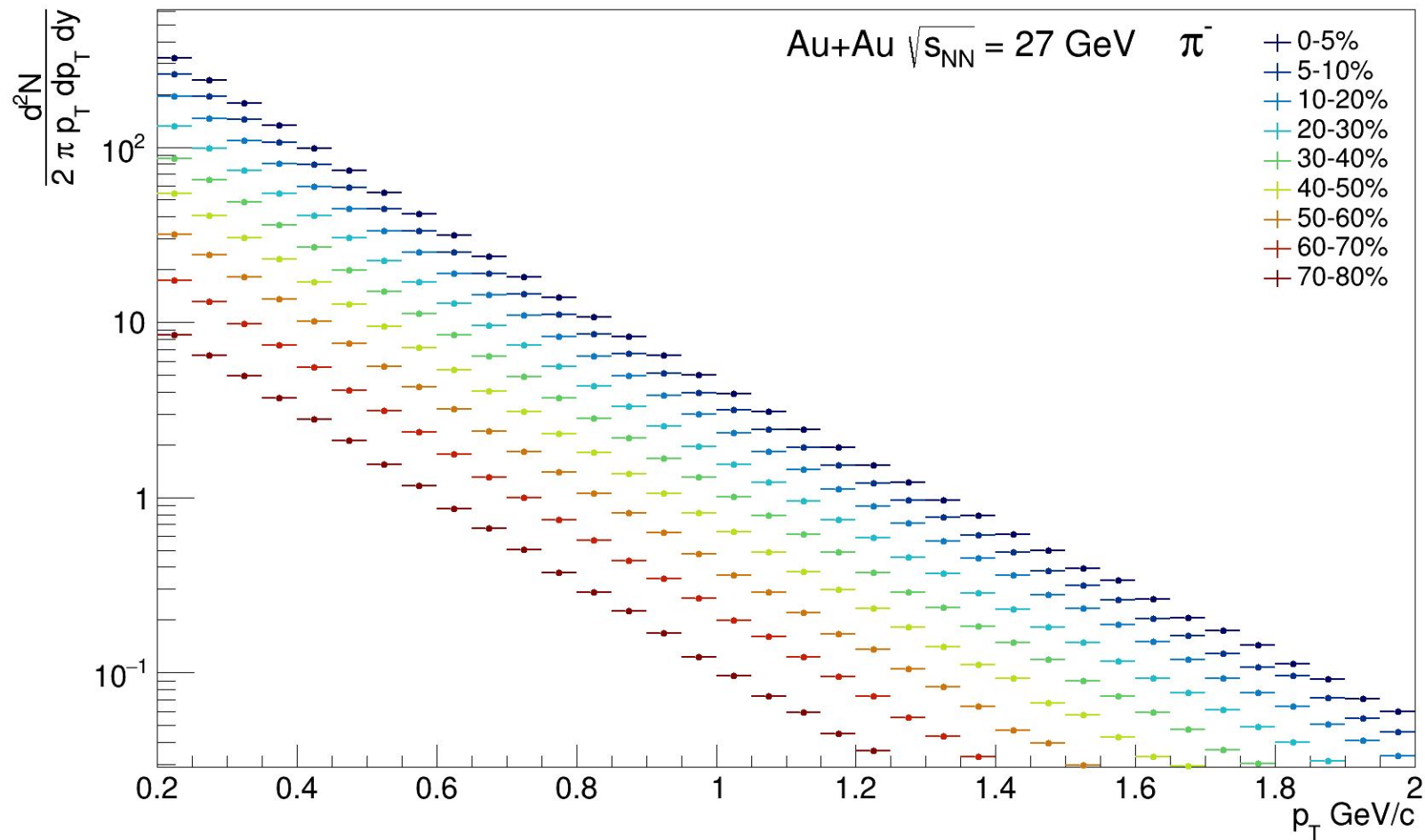
Bin width for spectra:  $50 \text{ MeV}/c$

Centrality was calculated using multiplicity.

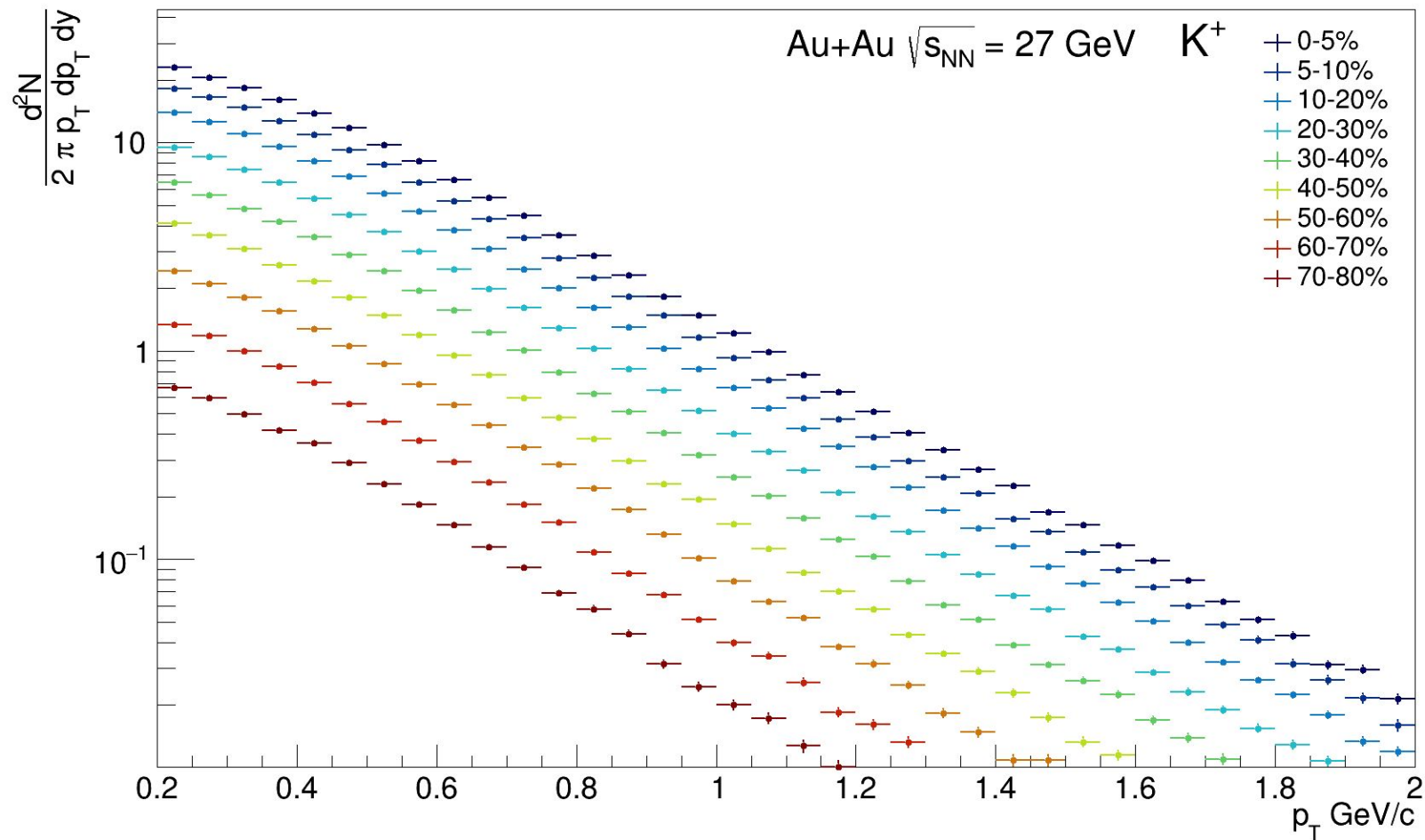
# Centrality dependence of $\pi^+$ spectra at $\sqrt{s_{\text{NN}}} = 27$ GeV



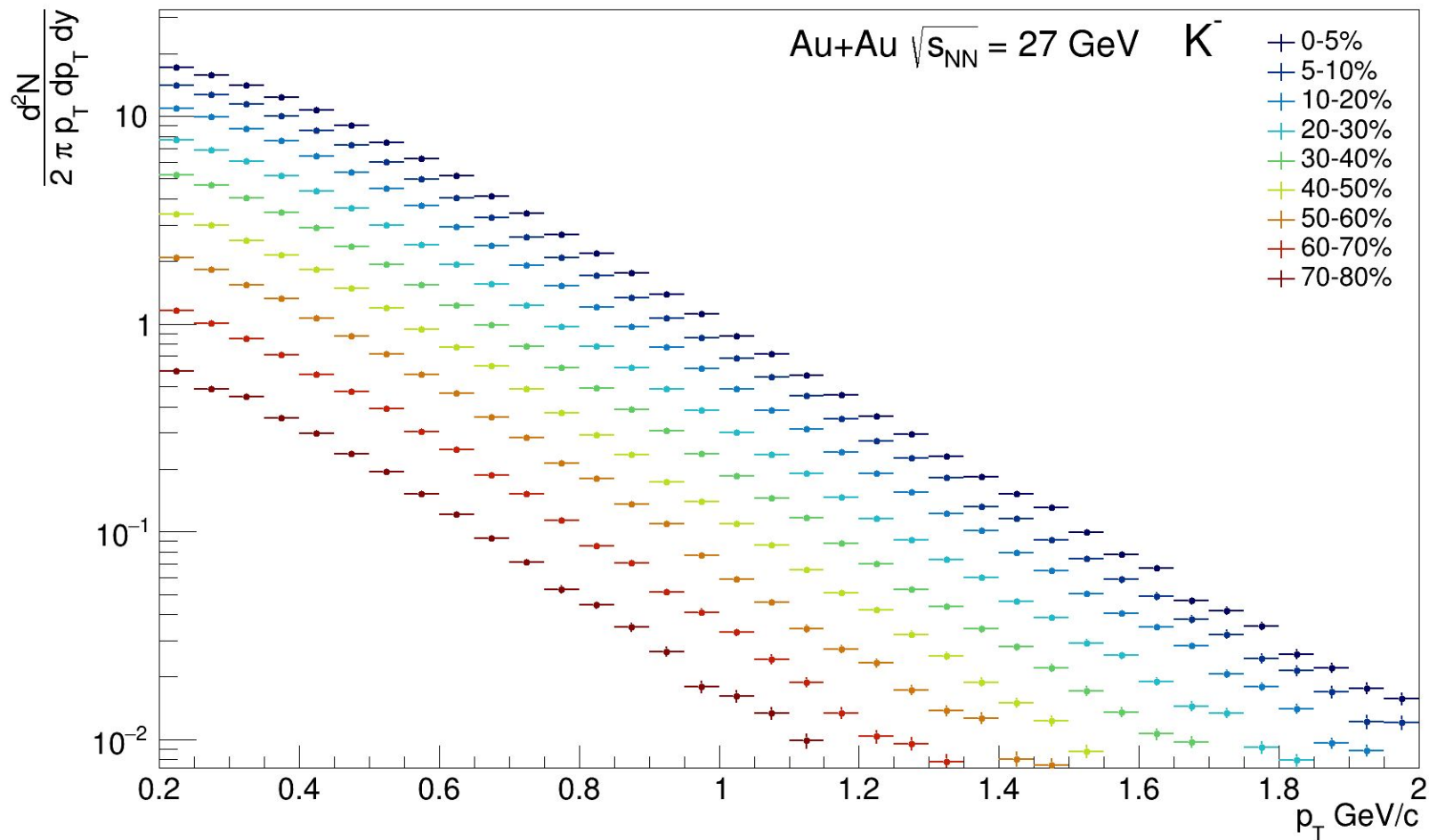
Centrality dependence of  $\pi^-$  spectra at  $\sqrt{s_{NN}} = 27$  GeV



Centrality dependence of  $K^+$  spectra at  $\sqrt{s_{NN}} = 27$  GeV

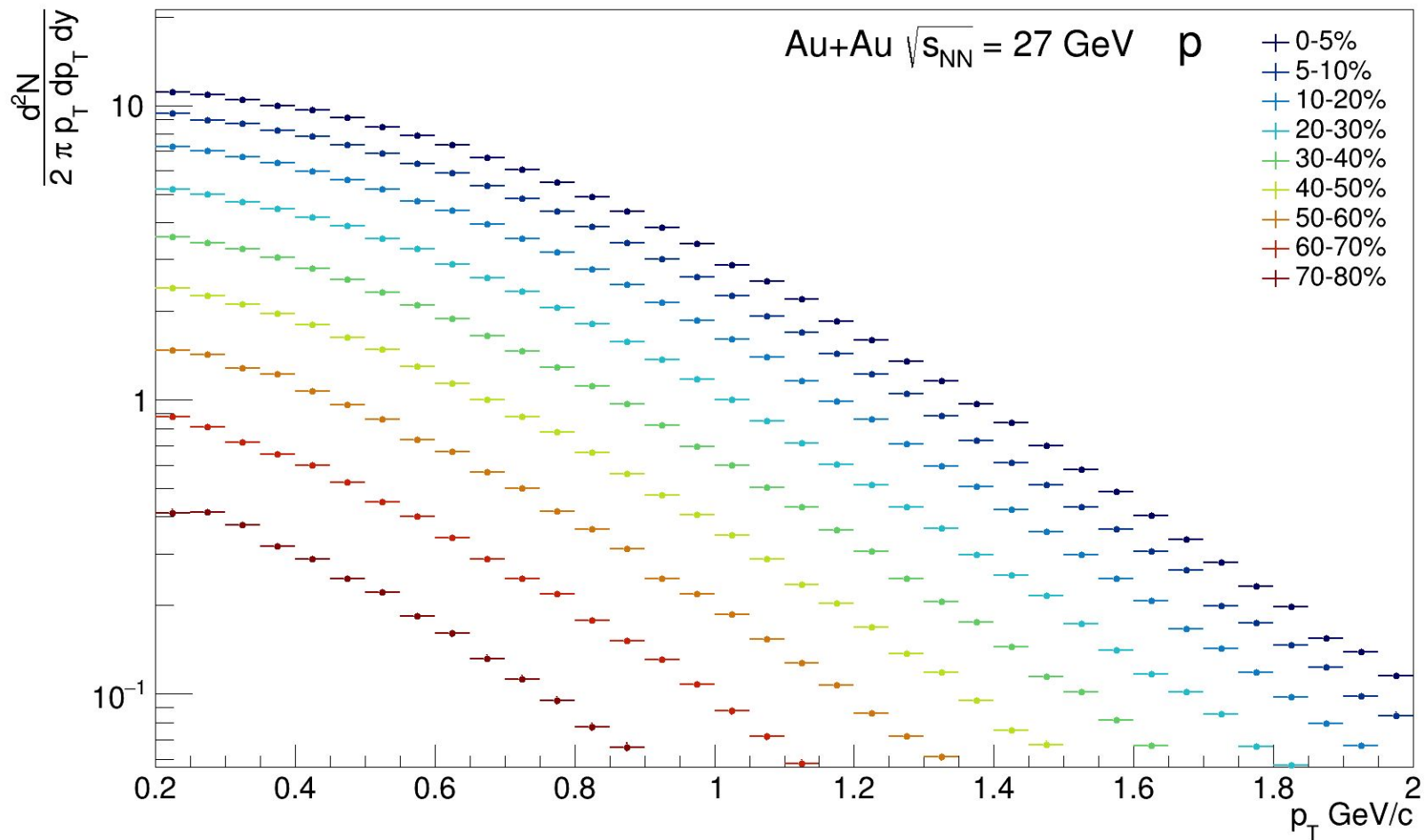


Centrality dependence of  $K^-$  spectra at  $\sqrt{s_{NN}} = 27$  GeV

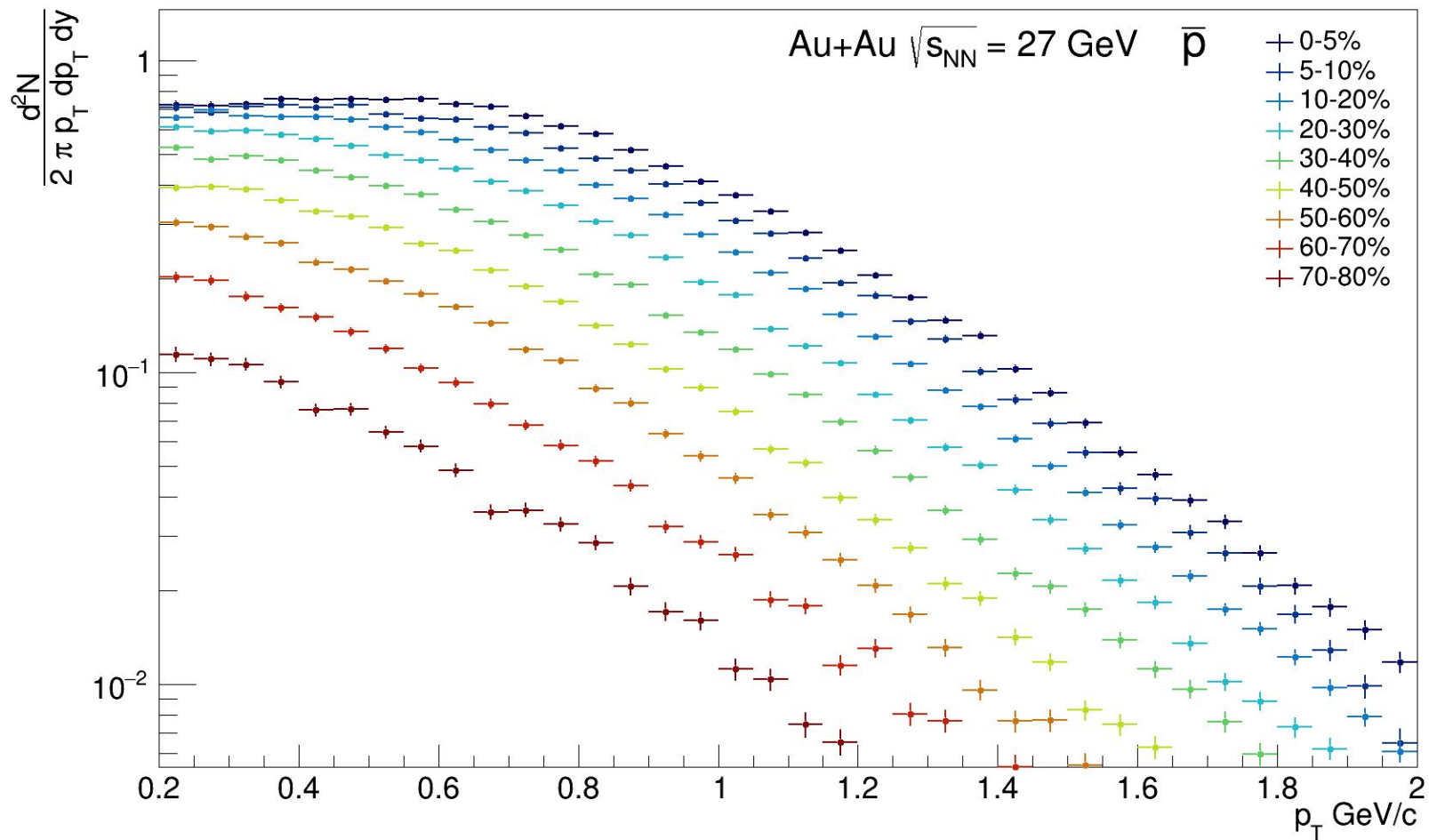




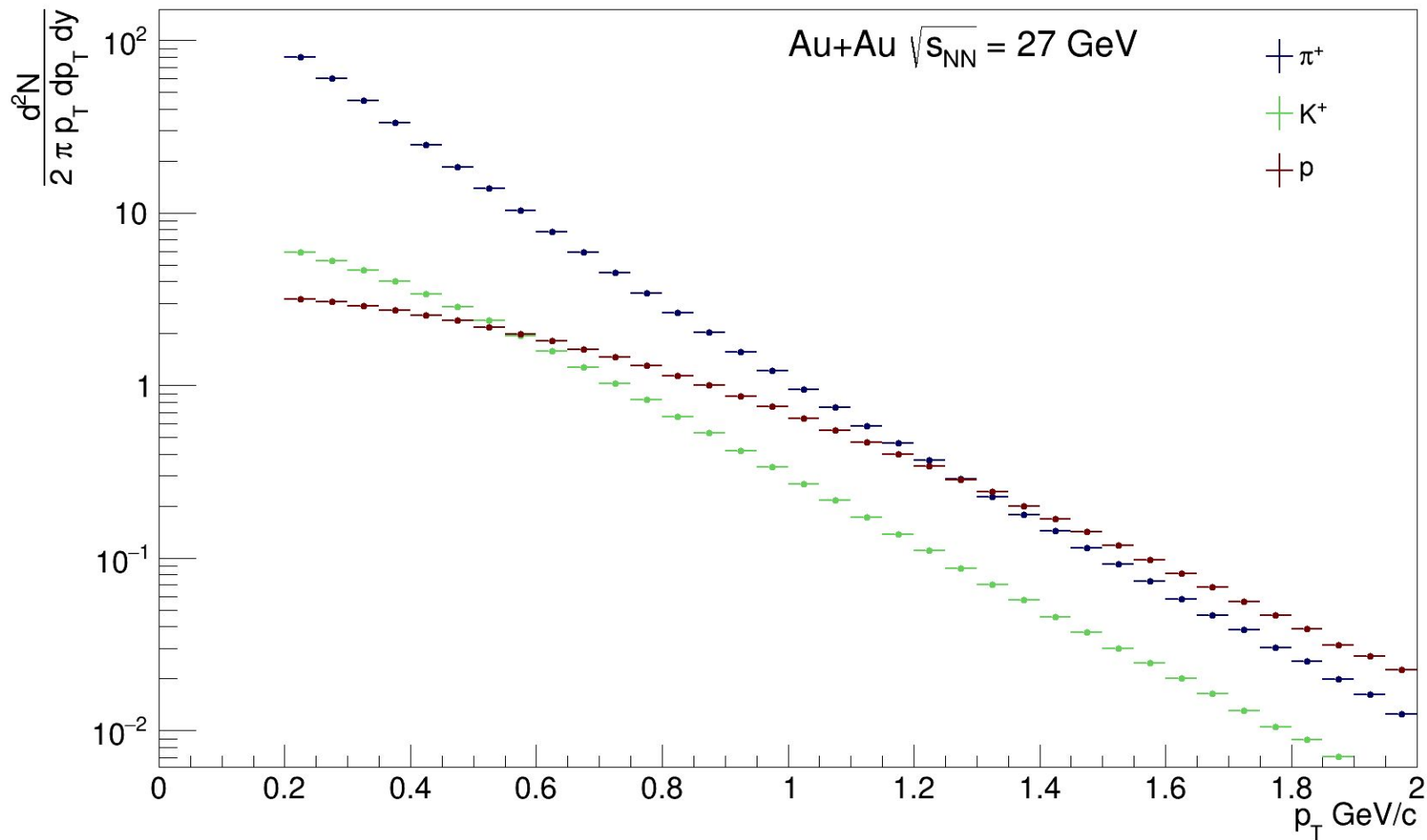
Centrality dependence of p spectra at  $\sqrt{s_{NN}} = 27$  GeV



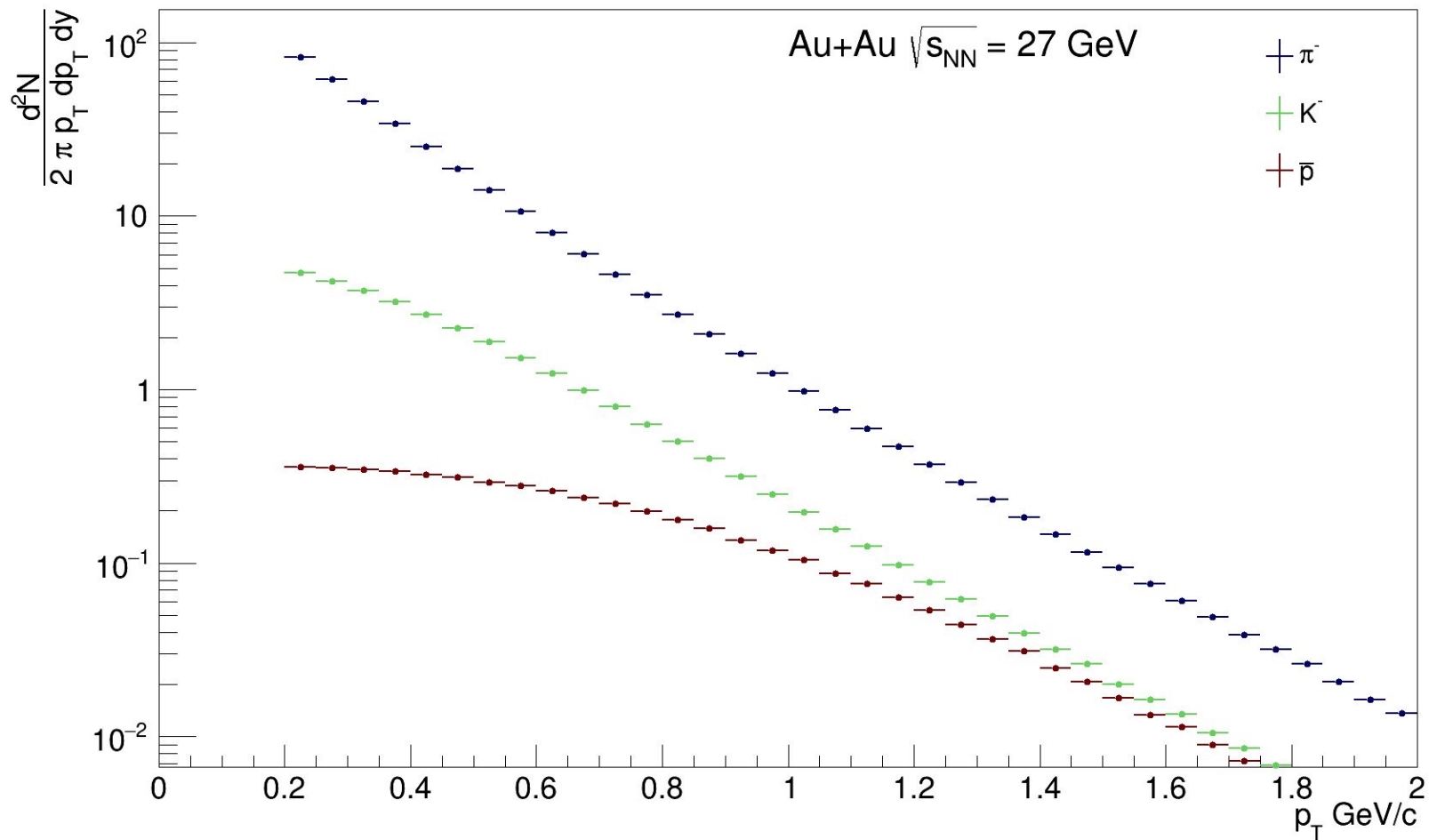
Centrality dependence of p-bar spectra at  $\sqrt{s_{NN}} = 27$  GeV



$\pi^+/\text{K}^+/\text{p}$  spectra at  $\sqrt{s_{\text{NN}}} = 27$  GeV in integrated centrality range



$\pi^-/K^-/p\text{-bar}$  spectra at  $\sqrt{s_{NN}} = 27$  GeV in integrated centrality range



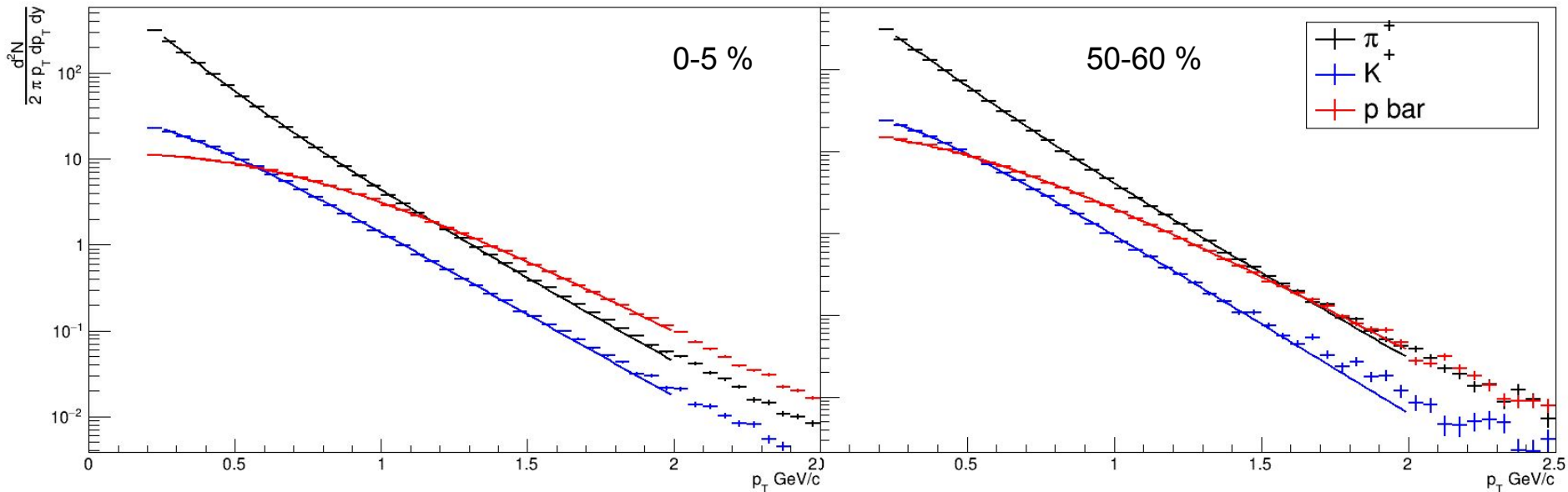
# blast wave fit

$$\frac{dN}{p_T dp_T} \propto \int_0^R r dr m_T I_0 \left( \frac{p_T \sinh \rho(r)}{T_{\text{kin}}} \right) \times K_1 \left( \frac{m_T \cosh \rho(r)}{T_{\text{kin}}} \right),$$

where  $m_T$  is the transverse mass of a hadron,  $\rho(r) = \tanh^{-1} \beta$ , and  $I_0$  and  $K_1$  are the modified Bessel functions. We use a radial flow velocity profile of the form

$$\beta = \beta_S (r/R)^n, \quad (14)$$

where  $\beta_S$  is the surface velocity,  $r/R$  is the relative radial position in the thermal source, and  $n$  is the exponent of flow velocity profile. Average transverse radial flow velocity  $\langle \beta \rangle$  can then be obtained from  $\langle \beta \rangle = \frac{2}{2+n} \beta_S$ .



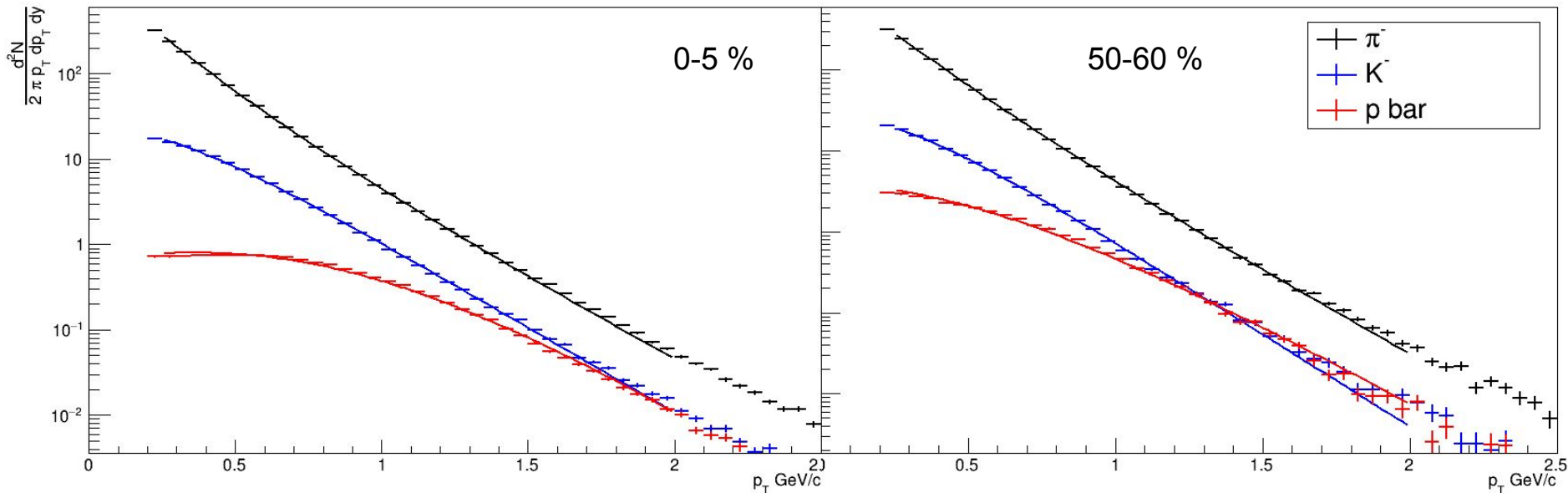
# blast wave fit

$$\frac{dN}{p_T dp_T} \propto \int_0^R r dr m_T I_0 \left( \frac{p_T \sinh \rho(r)}{T_{\text{kin}}} \right) \times K_1 \left( \frac{m_T \cosh \rho(r)}{T_{\text{kin}}} \right),$$

where  $m_T$  is the transverse mass of a hadron,  $\rho(r) = \tanh^{-1} \beta$ , and  $I_0$  and  $K_1$  are the modified Bessel functions. We use a radial flow velocity profile of the form

$$\beta = \beta_S (r/R)^n, \quad (14)$$

where  $\beta_S$  is the surface velocity,  $r/R$  is the relative radial position in the thermal source, and  $n$  is the exponent of flow velocity profile. Average transverse radial flow velocity  $\langle \beta \rangle$  can then be obtained from  $\langle \beta \rangle = \frac{2}{2+n} \beta_S$ .



	Centr	$\langle\beta\rangle$	$T_{\text{kin}}$ , MeV
Pion +	0-5 %	0.53	75.3
K +		0.32	140.6
p		0.45	111.8
Pion -		0.53	73.8
K -		0.24	156.6
p Bar		0.53	72.5
Pion +	50-60%	0.42	102.1
K +		0.31	119.9
p		0.26	153.7
Pion -		0.44	98.5
K -		0.31	116.7
p Bar		0.10	184.5

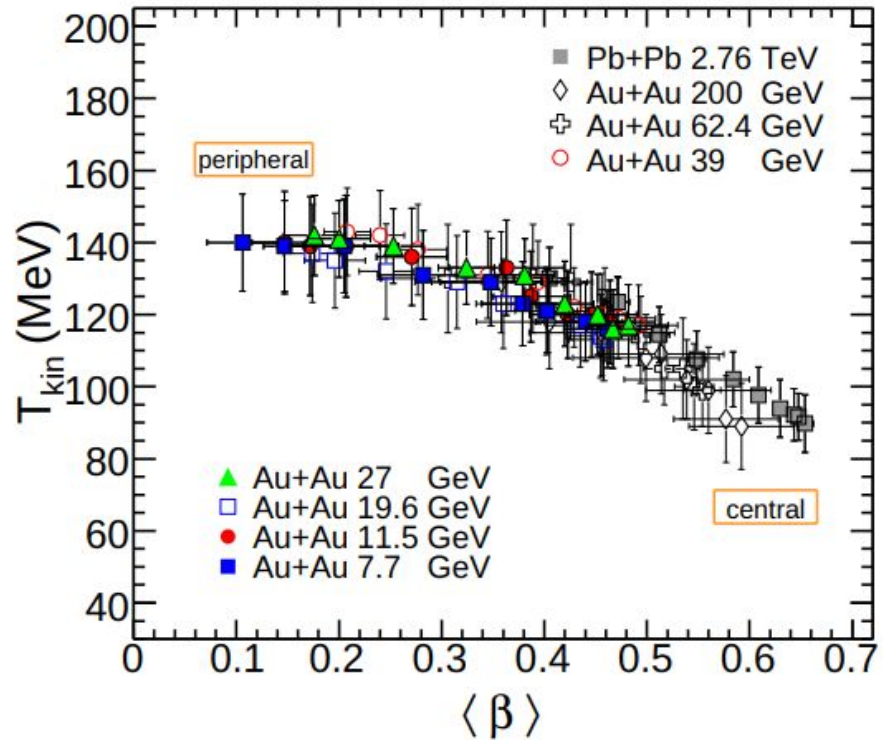


FIG. 37: (Color online) Variation of  $T_{\text{kin}}$  with  $\langle\beta\rangle$  for different energies and centralities. The centrality increases from left to right for a given energy. The data points other than BES energies are taken from Refs. [43, 66]. Uncertainties represent systematic uncertainties.